Cell Reports
Resource

SILAC Proteomics of Planarians Identifies Ncoa5 as a Conserved Component of Pluripotent Stem Cells

Alexander Böser,[1] Hannes C.A. Drexler,[2] Hanna Reuter,[1] Henning Schmitz,[1,3] Guangming Wu,[4] Hans R. Schöler,[4] Luca Gentile,[3] and Kerstin Bartscherer[1,*]
[1]Max Planck Research Group on Stem Cells and Regeneration, Max Planck Institute for Molecular Biomedicine, Von-Esmarch-Strasse 54, 48149 Münster, Germany
[2]Bioanalytical Mass Spectrometry Facility, Max Planck Institute for Molecular Biomedicine, Röntgenstrasse 20, 48149 Münster, Germany
[3]Planarian Stem Cell Laboratory, Max Planck Institute for Molecular Biomedicine, Von-Esmarch-Strasse 54, 48149 Münster, Germany
[4]Department for Cell and Developmental Biology, Max Planck Institute for Molecular Biomedicine, Röntgenstrasse 20, 48149 Münster, Germany
*Correspondence: kerstin.bartscherer@mpi-muenster.mpg.de
http://dx.doi.org/10.1016/j.celrep.2013.10.035

SUMMARY

Planarian regeneration depends on the presence of pluripotent stem cells in the adult. We developed an in vivo stable isotope labeling by amino acids in cell culture (SILAC) protocol in planarians to identify proteins that are enriched in planarian stem cells. Through a comparison of SILAC proteomes of normal and stem cell-depleted planarians and of a stem cell-enriched population of sorted cells, we identified hundreds of stem cell proteins. One of these is an ortholog of nuclear receptor coactivator-5 (Ncoa5/CIA), which is known to regulate estrogen-receptor-mediated transcription in human cells. We show that Ncoa5 is essential for the maintenance of the pluripotent stem cell population in planarians and that a putative mouse ortholog is expressed in pluripotent cells of the embryo. Our study thus identifies a conserved component of pluripotent stem cells, demonstrating that planarians, in particular, when combined with in vivo SILAC, are a powerful model in stem cell research.

INTRODUCTION

Planarian flatworms are known for their outstanding regenerative capacity that enables them to replace any missing body part from only a small piece of tissue. Regeneration is based on the presence of adult stem cells, also called neoblasts, which constitute about 25%–30% of all planarian cells (Baguna et al., 1989). Upon tissue loss, these stem cells are activated by thus-far-unknown mechanisms and accumulate at the wound where their descendants form the regeneration blastema (Eisenhoffer et al., 2008; Wenemoser and Reddien, 2010). The blastema is the site of massive differentiation, ultimately developing into the part of the body that has been lost upon injury. In uninjured animals, the stem cell pool is kept in equilibrium between cell division and differentiation, and, at least in some tissues, stem cell progeny constantly replace differentiated cells (Eisenhoffer et al., 2008; Forsthoefel et al., 2011; Lapan and Reddien, 2011; Pellettieri and Sánchez Alvarado, 2007).

Planarian stem cells are defined by their ability to proliferate, their morphology, and the expression of certain markers, such as the PIWI family member *smedwi-1*. Due to these characteristics, they can be depleted by γ-irradiation, sorted by fluorescence activated cell sorting (FACS), and detected in situ by antibodies and RNA probes (reviewed in Reddien, 2013). It has recently been shown that at least some planarian stem cells are pluripotent, as a single transplanted cell can rescue a stem cell-depleted individual (Wagner et al., 2011).

In mammals, pluripotency is limited to early embryos and is induced and maintained by a small number of key transcription factors. Among the most widely studied factors are Oct4 and Sox2, which can reprogram somatic cells into a pluripotent state (Kim et al., 2008, 2009; Takahashi et al., 2007). Recently it has been shown that the nuclear receptor Essrb functions in Oct4- and Sox2-mediated reprogramming of mouse embryonic fibroblasts (Feng et al., 2009) and that its coactivator, Nuclear Receptor Coactivator 3 (Ncoa3), is essential for both the induction and maintenance of pluripotency (Percharde et al., 2012; Wu et al., 2012).

Stem cell research lacks model organisms for observing and manipulating pluripotent stem cells in vivo. Planarians, containing many adult pluripotent stem cells, bear this potential; however, they are poorly characterized in terms of protein expression and lack analytical tools. In this study, we developed a metabolic labeling protocol for quantitative proteomics in planarians using stable isotope labeling by amino acids in cell culture (SILAC) (Ong et al., 2002). Applying this protocol, we identified hundreds of stem cell proteins by comparing the proteomes of untreated and irradiated planarians, and those of FACS-enriched stem cells. Among them, we found a protein similar to mammalian nuclear receptor coactivator 5 (Ncoa5). We show that planarian *ncoa5* is functionally required for stem cell-based regeneration

and maintenance of the planarian pluripotent stem cell pool, and that its mouse ortholog is expressed in the inner cell mass of the blastocyst, where pluripotent stem cells reside. Our study demonstrates that SILAC proteomics in combination with a highly plastic model organism such as planarian is a powerful tool for the identification of conserved stem cell proteins, the analysis of their turnover, and for the characterization of stem cell-based processes such as regeneration, in vivo.

RESULTS

Planarian Proteins Are Efficiently Labeled Using In Vivo SILAC

Analysis of gene expression in planarian stem cells has been performed mainly at the transcriptome level (Blythe et al., 2010; Galloni, 2012; Labbé et al., 2012; Onal et al., 2012; Resch et al., 2012; Shibata et al., 2012; Solana et al., 2012). However, posttranscriptional processing, translational rates, and protein turnover might cause large discrepancies between transcript and protein levels (Gygi et al., 1999). We set out to develop a sensitive method for detecting protein abundance and changes in protein levels in planarians. We reasoned that planarians might be especially susceptible for metabolic labeling due to their high plasticity and cell turnover rate (Newmark and Sánchez Alvarado, 2002; Pellettieri and Sánchez Alvarado, 2007). Thus, we used SILAC mouse liver labeled to >96% with the heavy isotope $^{13}C_6$-lysine (Krüger et al., 2008) to feed planarians of the species *Schmidtea mediterranea* (*Smed*) (Figure 1A). To determine the incorporation rate, proteins were extracted each week and analyzed by mass spectrometry (MS). After 1 week of feeding, 21% of all lysine residues were replaced by the heavy isotope-labeled amino acid, considering the 100 most intense proteins (Figure 1C). The incorporation rate increased to 88% after 11 weeks and reached >96% after 20 weeks of feeding (Figure 1C).

To ensure complete SILAC labeling also of tissues with a very slow turnover, we took advantage of the regenerative abilities of planarians. We reasoned that amputation would induce body-wide remodeling of tissues (Pellettieri et al., 2010), causing an increased turnover of proteins. In addition, relatively stable tissues would be labeled more efficiently if planarians had to form these tissues de novo during regeneration. Hence, we cut off the tail of planarians after feeding them with SILAC mouse liver for 6 weeks and let the tails regenerate to intact planarians. After an additional 23 weeks of feeding, we obtained an average labeling efficiency equivalent to the labeling of the SILAC mouse liver (>96%), suggesting that maximum labeling efficiency has been achieved (Figures 1B and 1C). We used lysates from these planarians as a spike-in standard in subsequent proteomics experiments.

Interestingly, the labeling efficiency of planarians was similar to that of *Caenorhabditis elegans* (up to 98%) and *Drosophila melanogaster* (up to 95%), invertebrate animals with relatively short generation times (Krijgsveld et al., 2003). Similarly, our results suggest that in planarians a high labeling efficiency can be achieved in a relatively short time, when compared to SILAC labeling of vertebrates (Konzer et al., 2013; Krüger et al., 2008; Looso et al., 2010; McClatchy et al., 2007; Westman-Brinkmalm et al., 2011). SILAC labeling did not affect the viability, growth, regeneration, and behavior of planarians (data not shown), demonstrating that labeling did not interfere with metabolic or other important processes in planarians.

SILAC Proteomics as a Tool to Study Planarian Protein Turnover

Amino acids are incorporated into newly made proteins during mRNA translation. As protein degradation and synthesis are in equilibrium under normal homeostatic conditions (reviewed in Rothman, 2010), incorporation rates of heavy amino acids should give a rough estimate of how fast proteins turnover during planarian tissue homeostasis. To investigate different incorporation rates of heavy amino acids into various proteins, we made use of the tissue samples collected weekly during the labeling procedure (Figure 1A) and compared the incorporation of heavy lysine residues into peptides of representative proteins that had been identified at all time points (Figure S1; Data S1). Our analysis revealed that this set of 295 sequences contains proteins with relatively fast incorporation times (50% labeling within 1 week), as exemplified by the stem cell-resident protein SMEDWI-1 (Figure 1D), and proteins with relatively slow incorporation rates (50% after > 6 weeks), such as proteins of the myosin family (Figure 1D), known to regulate important processes in muscles (reviewed in Berg et al., 2001). Exemplified by the mass spectra of heat shock protein 60 in Figure 1D, the majority of proteins analyzed revealed a minimum labeling efficiency of 50% after 4 weeks of labeling (Figures 1C and S1). Those results underscore the speed and effectiveness of in vivo SILAC labeling in planarians, and its potential to aid in future systematic investigations into planarian protein turnover, for instance, with a pulsed SILAC approach (Schwanhäusser et al., 2009). Nearly all 295 analyzed proteins were labeled to >90% after 14 weeks of labeling, suggesting that the majority of planarian proteins is turned over in less than 4 months.

SILAC Proteomics Identifies Stem Cell-Associated Proteins

Planarian stem cells can be eliminated by irradiation, as they are the only dividing cells in the entire organism (Reddien and Sánchez Alvarado, 2004). To extrapolate the stem cell proteome, we compared normal with irradiated planarians. Six days postirradiation (dpir), we extracted the proteins from irradiated and control animals (Figure 2A) and mixed the protein extracts with the SILAC spike-in standard, a protein extract prepared from SILAC planarians (Figure 1B), to allow direct comparison of the samples after MS analysis. In order to maximize the number of identified proteins, we used two distinct protein-processing methods, namely, one-dimensional SDS-PAGE and filter-assisted sample preparation protocol (FASP). Using the translated nucleotide sequence database of an in-house assembled *Schmidtea mediterranea* transcriptome as a reference (Data S2), we identified 3,741 proteins using the MaxQuant software package (Cox and Mann, 2008) (Data S3). The criterion for a sequence being counted was its detection with at least two peptides and at least one of them mapping uniquely to the sequence. Of those proteins, 3,376 were quantified in at least four of six biological replicates. This number is similar to

Cell PRESS
Open ACCESS

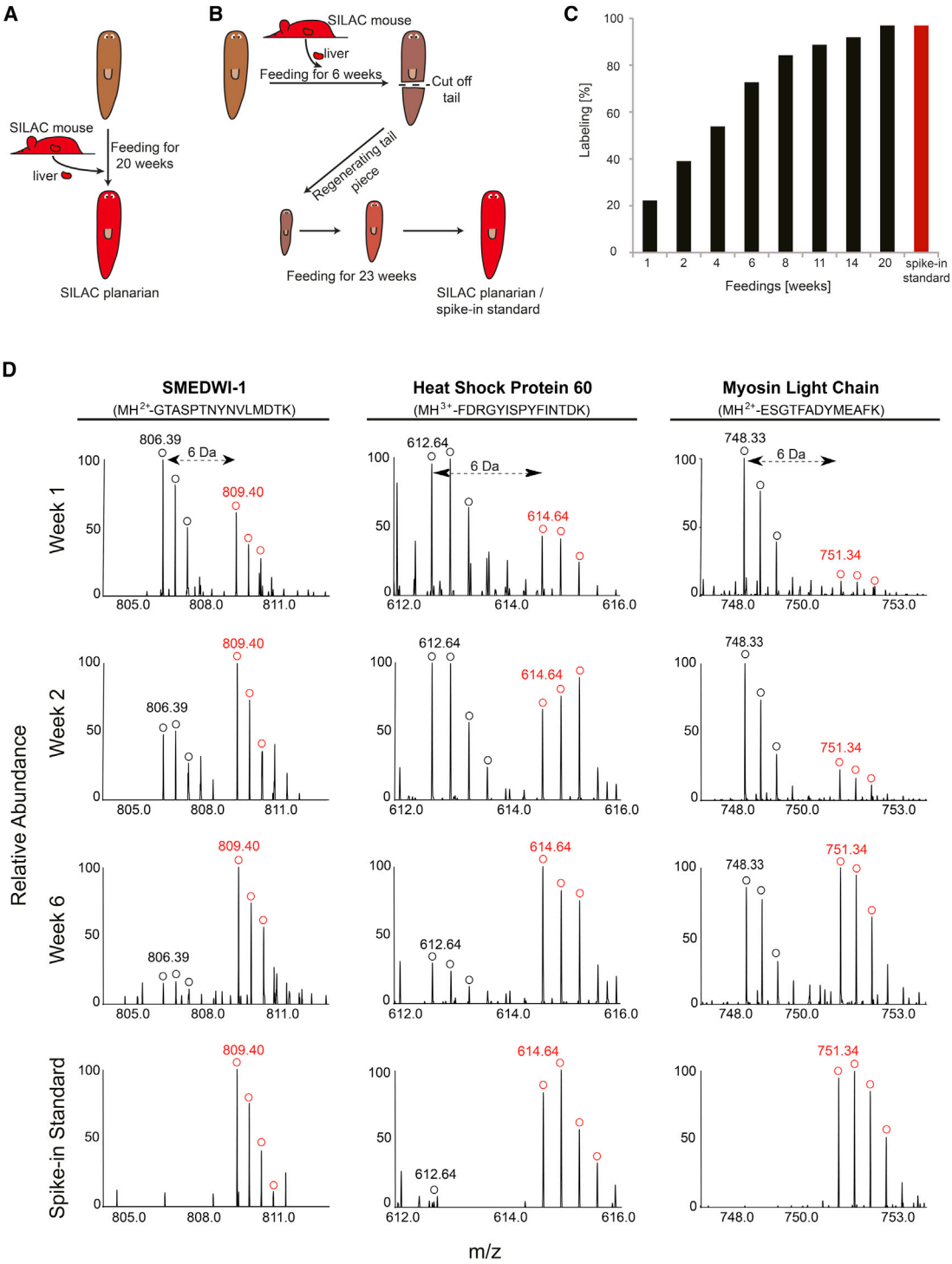

Figure 1. SILAC Labeling of Planarians

(A) SILAC labeling of planarians for the analysis of $^{13}C_6$-lysine incorporation into proteins.

(B) SILAC labeling of planarians for the generation of a spike-in standard. See text for details.

(C) Labeling efficiency over time. The red bar indicates the average labeling efficiency of the spike-in standard (>96%).

(D) Mass spectra of three peptides after 1, 2, and 6 weeks of feeding, and of the spike-in standard that led to the identification and quantification of SMEDWI-1, Heat Shock Protein 60, and Myosin Light Chain, respectively. Note the characteristic 6 Da shift between unlabeled light (black circles) and labeled heavy (red circles) isotope peak clusters. In the spike-in standard only the labeled peptide isotope clusters are detected. m/z, mass-to-charge ratio.

See also Figure S1 and Data S1.

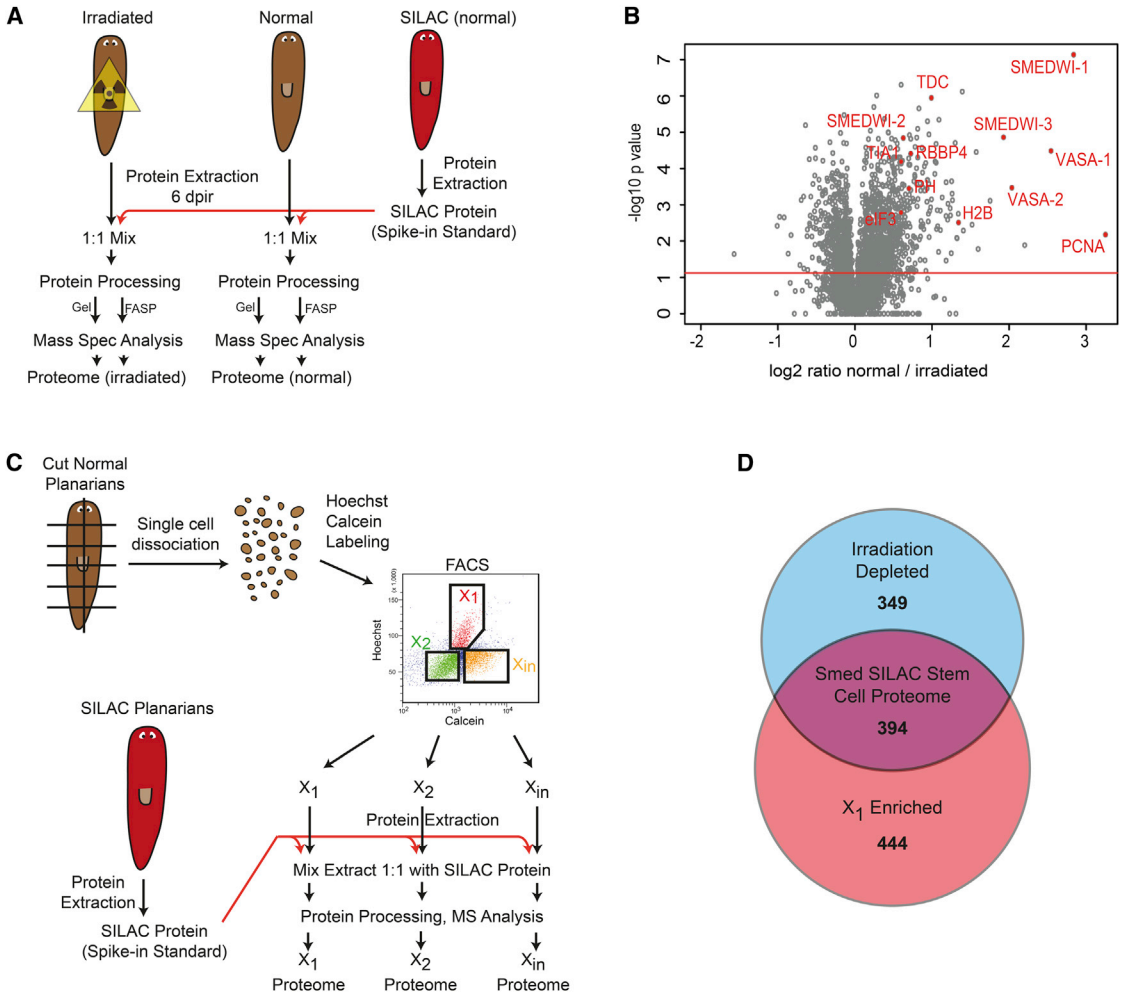

Figure 2. Identification of Stem Cell-Enriched Proteins with SILAC Proteomics

(A) Experimental set-up for the identification of stem cell-enriched proteins through SILAC proteomics of untreated and stem cell-depleted planarians by irradiation. See text for details.

(B) Volcano plot illustrating the log2 ratio of proteins from normal versus irradiated samples and their significance (−log10 p value). Known planarian stem cell-associated proteins are indicated in red.

(C) Experimental set-up for the identification of stem cell-enriched proteins by SILAC proteomics of FACS-sorted cells. The FACS plot used for gating and sorting of X_1, X_2, and X_{in} populations is illustrated in the scheme. See text for details.

(D) The Smed SILAC Stem Cell Proteome is the overlap between the irradiation and FACS X_1 data sets and includes 394 proteins.

See also Figure S2, Data S2, and Data S6.

other studies that have applied SILAC to whole organisms (Bonaldi et al., 2008; Konzer et al., 2013; Krüger et al., 2008; Looso et al., 2010). Statistical analysis showed that 743 proteins were either reduced or absent in stem cell-depleted animals (Figure 2B; Data S3).

In contrast, in a label-free experiment with identical experimental set-up but without addition of the SILAC spike-in standard, we quantified only 138 proteins as significantly enriched in the normal compared to the stem cell-depleted proteome, suggesting that SILAC labeling increased the sensitivity by a factor of 5 (Data S4). In addition, quantification by using SILAC was more precise compared to the label-free quantification approach (Figure S2A), similar to findings made in *Drosophila* (Sury et al., 2010).

As irradiation causes cellular stress and thus might induce stem cell-unrelated changes in gene expression, we validated our data set with an independent approach and sorted planarian stem cells by FACS (Hayashi et al., 2006; Reddien et al., 2005b) (Figure 2C). Cells were sorted into three different fractions according to their size and DNA content: an irradiation-sensitive fraction with high DNA content (>2n) consisting mainly of stem cells in S/G2/M phases of the cell cycle (X1), a partially irradiation-sensitive fraction with normal DNA content (2n) containing stem cells in G1 phase and small progeny (X2), and an irradiation-insensitive fraction with mainly differentiated cells (Xin) (Figure 2C). By SILAC proteomics, we quantified 2,680 proteins in X1 and Xin fractions, of which 838 proteins were enriched in X1, including many previously characterized stem cell proteins (Data S3).

Previous attempts to identify genes expressed in stem cells on the transcriptome level have discovered thousands of transcripts (Blythe et al., 2010; Eisenhoffer et al., 2008; Resch et al., 2012; Shibata et al., 2012; Solana et al., 2012; Wagner et al., 2012). We analyzed whether published transcriptome studies could confirm protein sequences we found with the SILAC approach, and whether our data set contained proteins not detected with these attempts. Hence, we obtained recently published *Schmidtea mediterranea* RNA sequencing (RNA-seq) data from irradiated animals (Solana et al., 2012), mapped them to our reference transcriptome, performed differential gene expression analysis using DESeq (Anders and Huber, 2010) (Data S5), and compared the set of differentially expressed sequences to our SILAC proteomics data set (Figure S2B). These analyses confirmed approximately 46% of the candidates from our irradiation experiment. Interestingly, 395 were exclusively identified by the SILAC approach.

This study is a comprehensive quantitative coverage of the planarian proteome; other studies are either based on 2D-DIGE or label-free approaches (Adamidi et al., 2011; Bocchinfuso et al., 2012; Fernández-Taboada et al., 2011; Onal et al., 2012). Considering the higher precision and sensitivity of the SILAC approach, we conclude that the use of metabolically labeled planarians is the method of choice for quantitative proteomics in planarians and possibly other highly plastic animals.

The *Smed* SILAC Stem Cell Proteome

We found that the SILAC irradiation and FACS data sets have 394 proteins in common (Figure 2D; Data S6). GO annotation analysis (Data S7) revealed that 19% of the proteins in this "core" proteomics data set were associated with "RNA binding" and 26% with "translation" (6% and 8% of the total set of identified proteins). This is consistent with previous studies and suggests that owing to the special importance that posttranscriptional processes may have in planarian stem cells (Fernandéz-Taboada et al., 2010; Rouhana et al., 2010, 2012), gene expression at the transcript level might not reflect the actual protein abundance.

To evaluate the quality of the data set, we searched for known planarian stem cell-associated proteins (Figure 2B) and found for example SMEDWI-1, proliferating cell nuclear antigen (PCNA), VASA-1, VASA-2, SMEDWI-2, SMEDWI-3, Histone2B (H2B), Retinoblastoma binding protein 4 (RBBP4), Eukaryotic translation initiation factor 3 (eIF3), and TIA1-like protein (TIA1), all of them conserved proteins that have been connected to planarian stem cells before (reviewed in Gentile et al., 2011; Wagner et al., 2012).

To further validate our data set, we selected 52 candidates from the set of 394 for in situ hybridization analysis (Figure 3). In addition to the proteins with the highest differences in protein abundance (Prot1–10), we exploited the whole range from high to relatively low differences in protein levels, included conserved and nonconserved sequences, and sequences with diverse GO annotations or no annotation at all (Table 1; Figure 3; Data S6), in order to get a broad and significant sampling.

Stem cells are located in a characteristic pattern between the gut branches in the parenchyma of planarians and can be visualized with a labeled RNA probe against *smedwi-1* mRNA (Sánchez Alvarado et al., 2002). Whole-mount in situ hybridization confirmed an irradiation-sensitive expression for most (43/52) candidate genes (Figure 3). Similarly to the stem cell marker *smedwi-1*, four genes (Prot4, 6, 12, 35) were expressed in an exclusive stem cell pattern, which was completely abolished 3 days after irradiation. However, the majority of genes were expressed in an irradiation-sensitive stem cell pattern and in irradiation-insensitive cells of the nervous system (Figure 3), similarly to the previously identified stem cell protein RBBP4 (Wagner et al., 2012). Expression in neurons has been described for most planarian stem cell genes; however, their function in these cells is not known (Rouhana et al., 2010).

Stem Cell-Associated Proteins Are Required for Proper Regeneration

In order to test if the SILAC proteome contains proteins with important function in stem cell-based regeneration, we chose ten proteins contained in the set of 52 for further analysis. We focused on proteins with obvious BLAST matches to conserved proteins that cover a broad spectrum of protein functions, ranging from chromatin remodeling (RUVBL1; CBX3), transcription (NCOA5/CIA; BTF3), posttranscriptional processing (SART3; THOC4; SNRNP200), to trafficking (FKBP6), and regulation of the cell cycle (SMC3; ARD1B). At least one of the ten candidates has been associated with pluripotent cells in other organisms (SART3) (Liu et al., 2012) (see Tables S1 and S2 for more details). Consistent with the loss of expression after irradiation, nine out of ten candidate genes showed reduced expression after *h2B* knockdown, an alternative treatment for the depletion of stem cells (Solana et al., 2012) (Figure S3A), five of them with a p value <0.05.

Loss of stem cells causes severe regeneration defects in planarians. In intact animals, depletion of stem cells leads to head regression, ventral curling, and subsequent lysis (Reddien et al., 2005a). Thus, we tested whether RNAi against our selected genes might cause similar phenotypes. We injected double-stranded RNA (dsRNA) against candidate mRNAs and amputated heads and tails from trunk pieces. Knockdown of nine candidate genes resulted in regeneration defects, ranging from loss of blastema formation to differentiation defects and lysis. The phenotypes were enhanced after a second amputation, because secondary wounds were closed but regeneration did not take place in most cases (Figure S3B).

In summary, our results indicate that the *Smed* SILAC Stem Cell Proteome, even though it may be smaller than published transcriptome data sets, is highly reproducible and contains stem cell-associated proteins with essential functions in planarian regeneration.

Ncoa5 Is Expressed in Stem Cells and Required for Maintenance of the Stem Cell Pool in Planarians

Among the tested SILAC candidates, we found a protein (Prot34) with sequence similarity (29% sequence identity) to the human Nuclear Receptor Coactivator 5 (NCOA5). Phylogenetic analysis revealed that Prot34 indeed clusters with vertebrate Ncoa5 family members, and not with those of the Ncoa3 family (Figure S4A). Similar to the human protein, which interacts with Estrogen Receptor alpha in cultured cells (Sauvé et al., 2001),

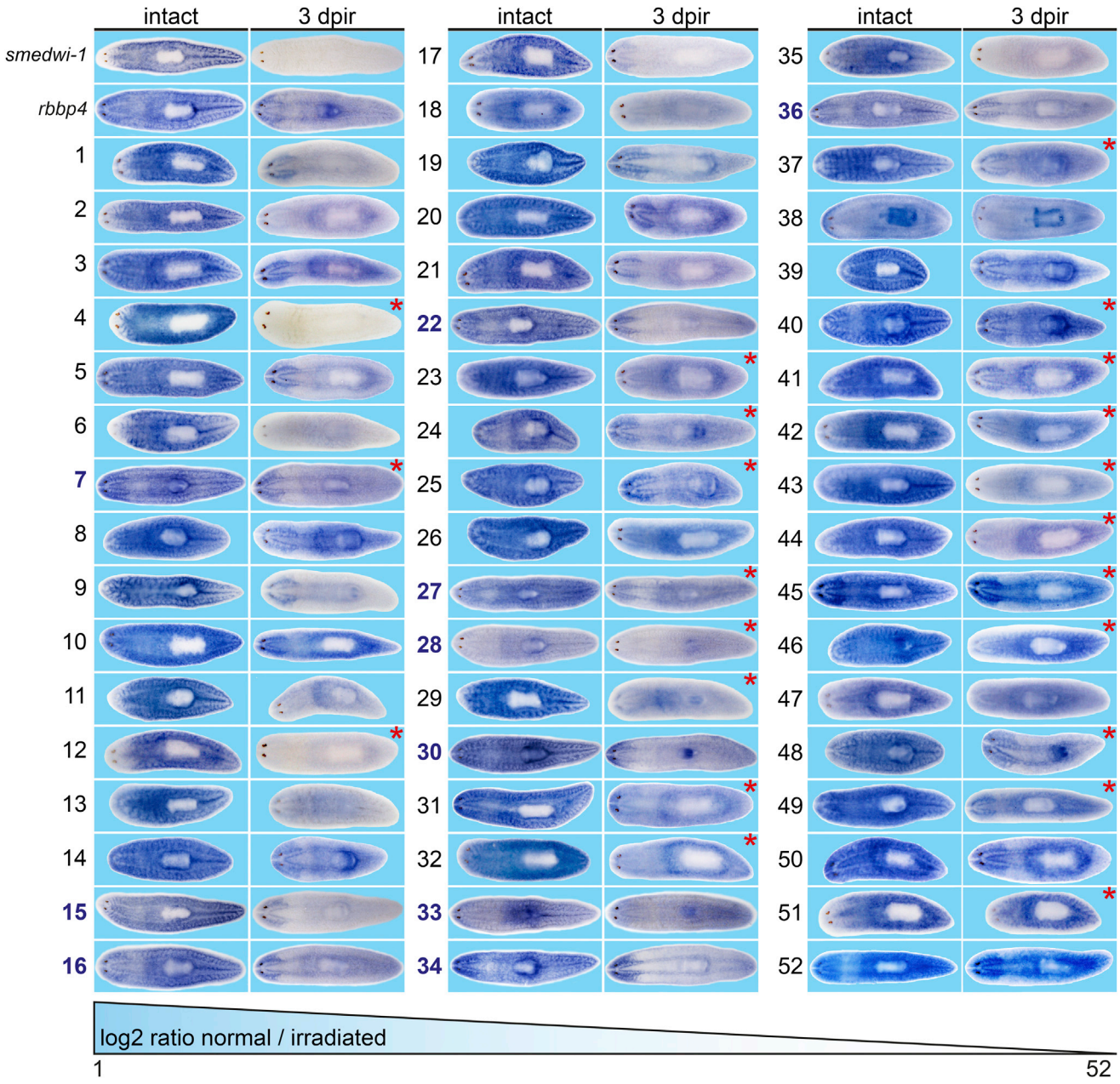

Figure 3. Validation of the Smed SILAC Stem Cell Proteome

Whole-mount in situ hybridization of 52 selected candidates in control planarians (left rows) and planarians 3 days after irradiation with 60 Gy (3 dpir, right rows). *smedwi-1* and *rbbp4* are positive controls. Candidates are sorted by their differences in protein levels between normal and irradiated animals (1 > 52). Red asterisks label candidates identified by SILAC proteomics but not by the analysis of transcriptome data (Solana et al., 2012). See text for details. Dark blue and bold numbers highlight the candidates that were selected for further validation by qPCR and RNAi-mediated gene knockdown. All animals were 2–4 mm in size. See also Figure S3 and Data S6.

planarian Ncoa5 contains an arginine- and aspartic acid-rich region, and a putative estrogen receptor interaction motif (Figure S4B) (Sauvé et al., 2001).

To confirm the expression of *ncoa5* in stem cells, we performed a double fluorescent in situ hybridization (FISH) together with a *smedwi-1* probe. We detected *ncoa5* in virtually all, *smedwi-1*$^{+}$ cells, and in some *smedwi-1*$^{-}$ cells, especially in the region of the planarian brain (Figure 4A). As for many stem cell genes, possibly owing to their similarity to germline stem cells (Solana, 2013), *ncoa5* was also expressed in testes of sexual *Schmidtea mediterranea* (Figure S5), demonstrating an expression profile typical for planarian stem cell genes.

RNAi against *ncoa5* led to severe impairment of regeneration, as fragments were not able to form an expanding blastema

Table 1. Top BLAST Hits of Selected Candidates

Protein No.	SRG12 No.	BLAST (nr)	Accession No.
1	29413	predicted: ribonucleoside-diphosphate reductase large subunit-like (*Ceratitis capitata*)	XP_004537904.1
2	42038	replication protein A (*Schistosoma mansoni*)	XP_002579153.1
3	22222	predicted: replication protein A 70 kDa DNA-binding subunit (*Melopsittacus undulatus*)	XP_005154512.1
4	19893	predicted: histone H2A-like (*Acyrthosiphon pisum*)	XP_003241023.1
5	32145	leucine-rich repeat and WD repeat-containing protein 1 (*Clonorchis sinensis*)	GAA51994.1
6	45088	putative dUTP pyrophosphatase (*Taeniopygia guttata*)	NP_001232536.1
7	37844	peptidyl prolyl *cis trans* isomerase FKBP-2, partial (*Schmidtea mediterranea*)	AFJ24780.1
9	22560	hypothetical protein BRAFLDRAFT_239771 (*Branchiostoma floridae*)	XP_002605562.1
10	24547	Y box protein-1, partial (*Schmidtea mediterranea*)	AFJ24764.1
12	26249	nucleolar protein NOP56 (*Schistosoma mansoni*)	XP_002576320.1
13	31757	SUMO-activating enzyme subunit 2 (*Crassostrea gigas*)	EKC24155.1
14	21623	hypothetical protein (*Schmidtea mediterranea*)	AFJ24787.1
15	16009	heterochromatin protein 1-like protein 1 (*Schmidtea mediterranea*)	AFL48187.1
16	40371	structural maintenance of chromosomes protein 3 (*Crassostrea gigas*)	EKC20316.1
17	32151	nuclear pore membrane glycoprotein gp210-related (*Schistosoma mansoni*)	XP_002575132.1
18	16001	transcription factor A mitochondrial (*Clonorchis sinensis*)	GAA27387.2
20	31037	predicted: serrate RNA effector molecule homolog isoform 1 (*Acyrthosiphon pisum*)	XP_001950813.2
21	27588	predicted: CCR4-NOT transcription complex subunit 10-like (*Amphimedon queenslandica*)	XP_003382418.1
22	12413	transcriptional coactivator (*Clonorchis sinensis*)	ABW89022.1
23	12157	hypothetical protein CAPTEDRAFT_164217 (*Capitella teleta*)	ELU01671.1
25	14474	SJCHGC00455 protein (*Schistosoma japonicum*)	AAW27073.1
27	33048	transcription factor BTF3 homolog 4 (*Salmo salar*)	ACI69109.1
28	12270	N-terminal acetyltransferase complex ard1 subunit (*Schistosoma mansoni*)	XP_002576366.1
29	35239	SJCHGC06672 protein (*Schistosoma japonicum*)	AAW26757.1
30	26662	predicted: ruvB-like 1-like (*Aplysia californica*)	XP_005106590.1
31	22671	fragile X mental retardation protein (*Dugesia japonica*)	ADF47425.1
32	12508	GTP-binding nuclear protein RAN/TC4 (*Brugia malayi*)	XP_001900408.1
33	31991	predicted: squamous cell carcinoma antigen recognized by T cells 3-like (*Bombus impatiens*)	XP_003494159.1
34	26496	hypothetical protein (*Schistosoma mansoni*)	XP_002570058.1
35	21991	coiled-coil domain-containing protein 25, partial (*Clonorchis sinensis*)	GAA51499.1
36	37503	predicted: U5 small nuclear ribonucleoprotein 200 kDa helicase (*Echinops telfairi*)	XP_004704418.1
37	38566	hypothetical protein (*Schistosoma mansoni*)	XP_002572826.1
39	27932	predicted: splicing factor U2AF 65 kDa subunit-like isoform 3 (*Oreochromis niloticus*)	XP_003442645.1
40	28993	Huntingtin-interacting protein K (*Clonorchis sinensis*)	GAA42879.1
41	30067	conserved hypothetical protein (*Phytophthora infestans* T30-4)	XP_002997685.1
42	31155	hypothetical protein SINV_12257 (*Solenopsis invicta*)	EFZ10687.1
43	24609	predicted: GTP-binding protein 128up-like (*Aplysia californica*)	XP_005108025.1
44	22370	mitochondrial ribosomal protein L43 (Spirometra erinaceieuropaei)	AFM74201.1
45	35172	predicted: zinc finger matrin-type protein 4-like (*Xenopus* (*Silurana*) *tropicalis*)	XP_002936484.2
47	16442	hypothetical protein TRIADDRAFT_56335 (*Trichoplax adhaerens*)	XP_002112383.1
48	38804	ferritin (*Rhipicephalus microplus*)	AAQ54710.1
51	33620	estradiol 17-beta-dehydrogenase 12 (*Xenopus* [Silurana] *tropicalis*)	NP_001017234.1

Orthologous protein sequences of the 52 selected candidates presented in Figure 3 were determined using BLASTp against the NCBI nonredundant database. SRG12 proteome identifiers, top BLAST hits (BLAST [nr]), and accession numbers of the BLAST hits are indicated. Proteins without a BLAST hit are excluded. See also Figure 3 and Data S6.

(30/30 fragments) (Figure 4B). In addition, several fragments (7/30) lysed within 10 days postamputation (dpa), and intact animals were dead within 14 days after the last injection (dpin) (Figure 4C). To identify the cause for impaired regeneration and ultimate death of the animals, we analyzed the presence of stem cells after *gfp*, *h2b*, or *ncoa5* knockdown at 7 dpa by flow cytometry. Although in control animals (*gfp* RNAi) we found about 24% of all single cells in the X1 fraction, RNAi against either *h2b* or

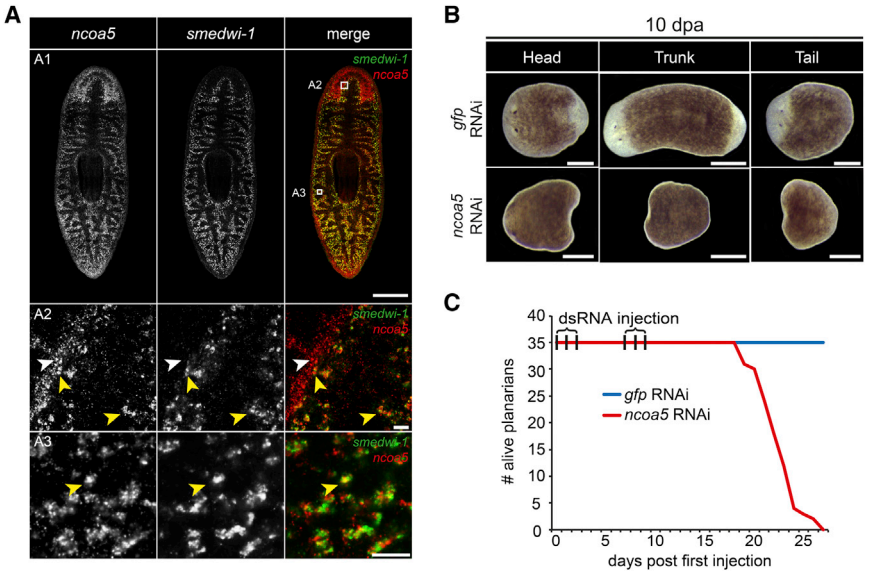

Figure 4. Prot34, an Ncoa5 Ortholog, Is Expressed in Planarian Stem Cells, and Required for Regeneration and Homeostasis

(A) Double FISH of *ncoa5* and the stem cell marker *smedwi-1*. (A1) Whole animals. (A2) Zoom-in in the brain region. (A3) Zoom-in near the pharynx. White arrowheads highlight *smedwi-1*$^{-}$/*ncoa5*$^{+}$ cells; yellow arrowheads point at double-positive cells. Scale bars: A1: 500 μm; A2, A3: 15 μm. Anterior is to the top.

(B) Regenerating head, trunk, and tail pieces of *gfp* or *ncoa5* RNAi animals 10 days postamputation (dpa). Scale bars: 1 mm. Anterior is to the left.

(C) Survival curves of homeostatic *gfp* or *ncoa5* RNAi animals.

See also Figures S4 and S5.

ncoa5 resulted in a reduced X1 population of 2% or 8% (Figure 5A), suggesting that the population of cycling stem cells was reduced.

To further confirm this finding, we analyzed *smedwi-1* expression by FISH of intact (Figure 5B) and regenerating planarians (Figures 5C and S6A) after *ncoa5* RNAi. Interestingly, *smedwi-1*$^{+}$ cells were almost entirely lost 8 days after the last dsRNA injection in intact animals, explaining the lethal RNAi phenotype of homeostatic planarians. Similarly, we detected fewer *smedwi-1*$^{+}$ cells in regenerating *ncoa5* RNAi animals than in controls, and none by 10 dpa. Double FISH of *smedwi-1* and *PC2*, a pan-neuronal marker (Agata et al., 1998), revealed that RNAi fragments were able to develop small brain tissues (Figure 5C), indicating that stem cells could still differentiate.

To test whether stem cells depleted of *ncoa5* could also proliferate, we used a mitosis-specific marker, an antibody against phospho-Histone 3 (Ser10) (Hendzel et al., 1997) at 3 dpa, when stem cells were still present. Immunostaining detected mitotically active cells in both *gfp* and *ncoa5* RNAi animals (Figures 5D, S6B, and S6D), demonstrating that stem cell proliferation was still taking place. Analogously, TUNEL staining of regenerating RNAi animals at 3 dpa and homeostatic RNAi animals at 4 dpin did not reveal any difference between *ncoa5* and control RNAi, suggesting that the loss of stem cells in *ncoa5* RNAi animals was not due to an increased apoptotic rate (Figures S6C and S6E).

Planarian stem cells can repopulate an animal whose own stem cells have been depleted by irradiation and rescue its regenerative abilities. After transplantation, stem cells are detected in the parenchyma of the host where they engraft, proliferate, and differentiate (Wagner et al., 2011, 2012). To test whether *ncoa5* RNAi animals were able to replenish the stem cell pool of an irradiated animal, we FACS-sorted stem cells (X1 population) from *ncoa5* RNAi planarians and injected approximately 1,500 cells into the postpharyngeal parenchyma of an irradiated host. Although control stem cells repopulated many irradiated host animals (11/32), we did not find any *smedwi-1*$^{+}$ stem cells and *NB.32.1g*$^{+}$ early stem cell progeny (Eisenhoffer et al., 2008), nor was there any mitotic activity in host animals injected with X1 cells from *ncoa5* RNAi animals (34/34) after 1 week. This suggests that stem cells are incapable of repopulating an irradiated host (Figure 5E).

Mouse Ncoa5 Is Expressed in the Pluripotent Inner Cell Mass of the Blastocyst

To test whether Ncoa5 is also expressed in the pluripotent cells of mammals, we analyzed its expression during mouse preimplantation development. Here, the blastomeres of the mouse embryo turn from totipotent (zygote: 4-cell stage) to pluripotent (8-cell morula stage) and eventually, after compaction and cavitation, segregate into multipotent trophectoderm (TE) and pluripotent inner cell mass (ICM) (Figure 6A). As shown in Figure 6B, *Ncoa5* was highly expressed in both unfertilized and fertilized eggs (peak of expression). Along with cleavage, its expression reached a minimum at the 4-cell stage (2.4% ± 0.6% of the peak). After the maternal-to-zygotic transition (MZT), which starts with the activation of the zygotic genome at the 2-cell stage (Schultz, 2002), zygotic *Ncoa5* expression was activated and increased to peak at the expanded blastocyst stage (34.4% ± 3.5% at 4.0 dpc). Notably, *Ncoa5* expression dynamics were similar to that of *Oct4*, but different from that of *Cdx2* (Figure 6B), a TE-restricted and exclusively zygotic gene (Strumpf et al., 2005).

Next, we determined the expression pattern of *Ncoa5* at both morula and blastocyst stages. Transcripts were found in all blastomeres of 3.0 dpc morulae, whereas in 4.0 dpc blastocysts they were restricted to the ICM (Figure 6C). Ncoa5 protein was similarly detected in all blastomeres of 3.0 dpc morulae (Figure 6D), but mainly in the ICM of 4.0 blastocysts (Figure 6E). Expression was strongly reduced after injection of small interfering RNAs (siRNAs) against *Ncoa5* into the mouse embryo (Figure S7A), suggesting that the antibody specifically detects Ncoa5 protein. Despite efficient knockdown of *Ncoa5* at 3.5 dpc, we did not detect any morphological abnormalities of embryos after siRNA

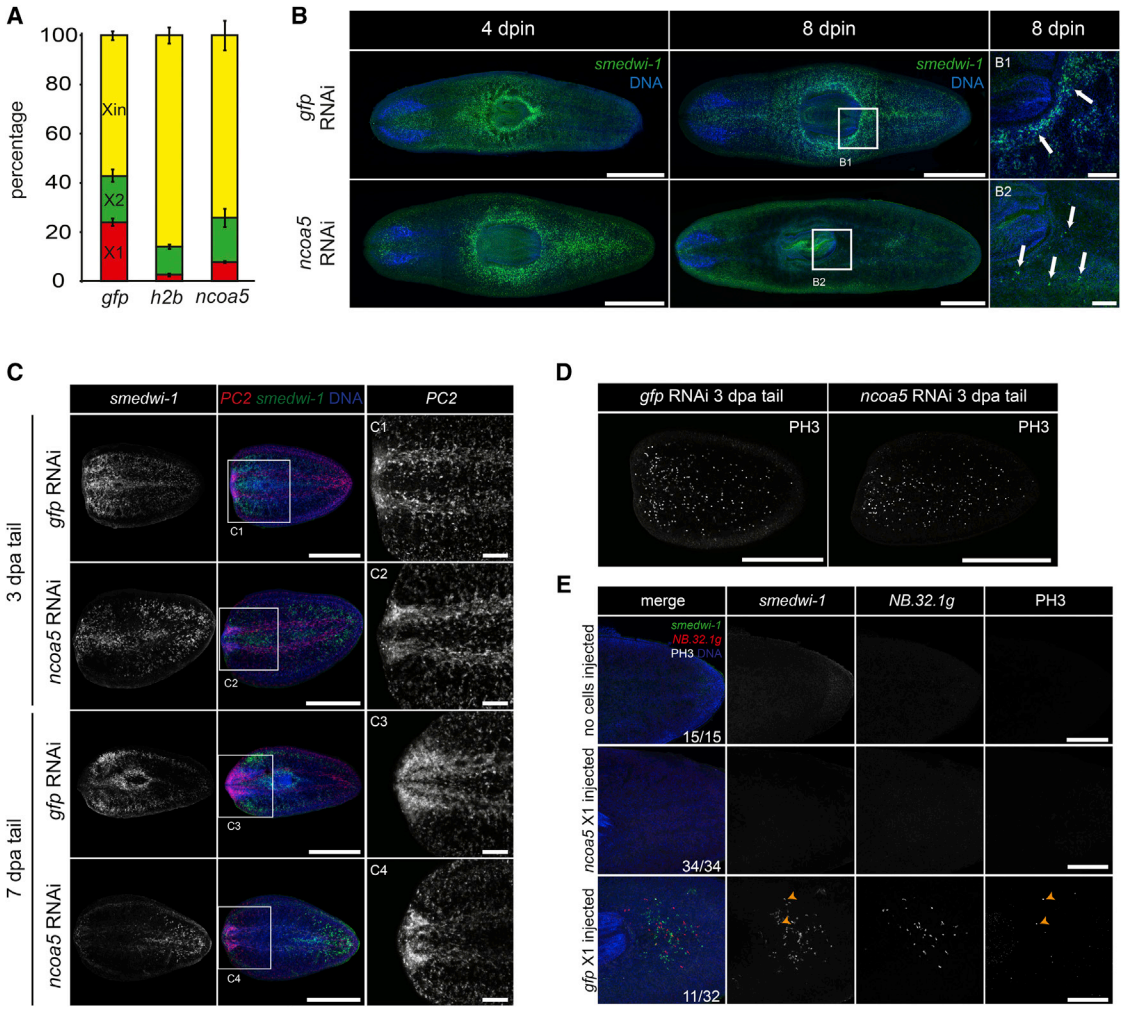

Figure 5. *Ncoa5* Is Required for the Maintenance of the Planarian Stem Cell Pool

(A) Flow cytometry analysis of *gfp*, *h2b*, or *ncoa5* RNAi animals 7 dpa. Error bars represent SD of three biological replicates.

(B) Homeostatic *gfp* or *ncoa5* RNAi animals at 4 or 8 days post last injection (dpin). (B1 and B2) Zoom-in in area with *smedwi-1*$^{+}$ cells, highlighted by white arrows. Scale bars: 500 μm (B) or 50 μm (B1 and B2).

(C) Regenerating tail pieces of *gfp* or *ncoa5* RNAi animals at 3 and 7 dpa. Double FISH of *smedwi-1* (stem cells) and *PC2* (neuronal cells). (C1–C4) Zoom-in in the anterior region where new cephalic ganglia form. Scale bars, 500 μm (C) and 100 μm (C1–C4).

(D) PH3 antibody staining of proliferating cells in *gfp* or *ncoa5* RNAi regenerating tail pieces at 3 dpa. Scale bars, 500 μm.

(E) Cell transplantation experiments. Approximately 1,500 stem cells isolated by FACS (X1 population) from *gfp* or *ncoa5* RNAi animals (4 dpin) were injected into lethally irradiated planarians (80 gy, 3 dpir). Stem cell presence, differentiation, and proliferation capabilities were analyzed 7 days after injection, using *smedwi-1* and *NB.32.1g* double FISH combined with PH3 antibody staining. Scale bars, 200 μm. Anterior is to the left.

See also Figure S6.

injections, possibly due to an unstable siRNA knockdown allowing full recovery of *Ncoa5* levels as early as 4.5 dpc (Figure S7B). Hence, stable genetic approaches will be required to pursue further investigations into *Ncoa5* function in early mouse development.

DISCUSSION

For our SILAC experiments, two populations of planarians were generated: one fed with SILAC mouse liver as a source of the heavy amino acid $^{13}C_6$-lysine and one fed with normal mouse liver as a supply of natural amino acids. During several weeks of feeding, planarians incorporated amino acids from their diet into newly synthesized proteins (Figure 1), generating "heavy" and "light" populations of planarians. What are the benefits of feeding SILAC mouse liver, a relatively expensive diet? Previous studies have shown that differential protein expression detected by mass spectrometry is most accurate if a peptide is directly compared with its stable isotope analog (Ong and Mann, 2005). Consistent with this, our comparison between SILAC and label-free quantification of a similar experimental set-up revealed a 5-fold higher sensitivity after labeling (Figure S2A). This

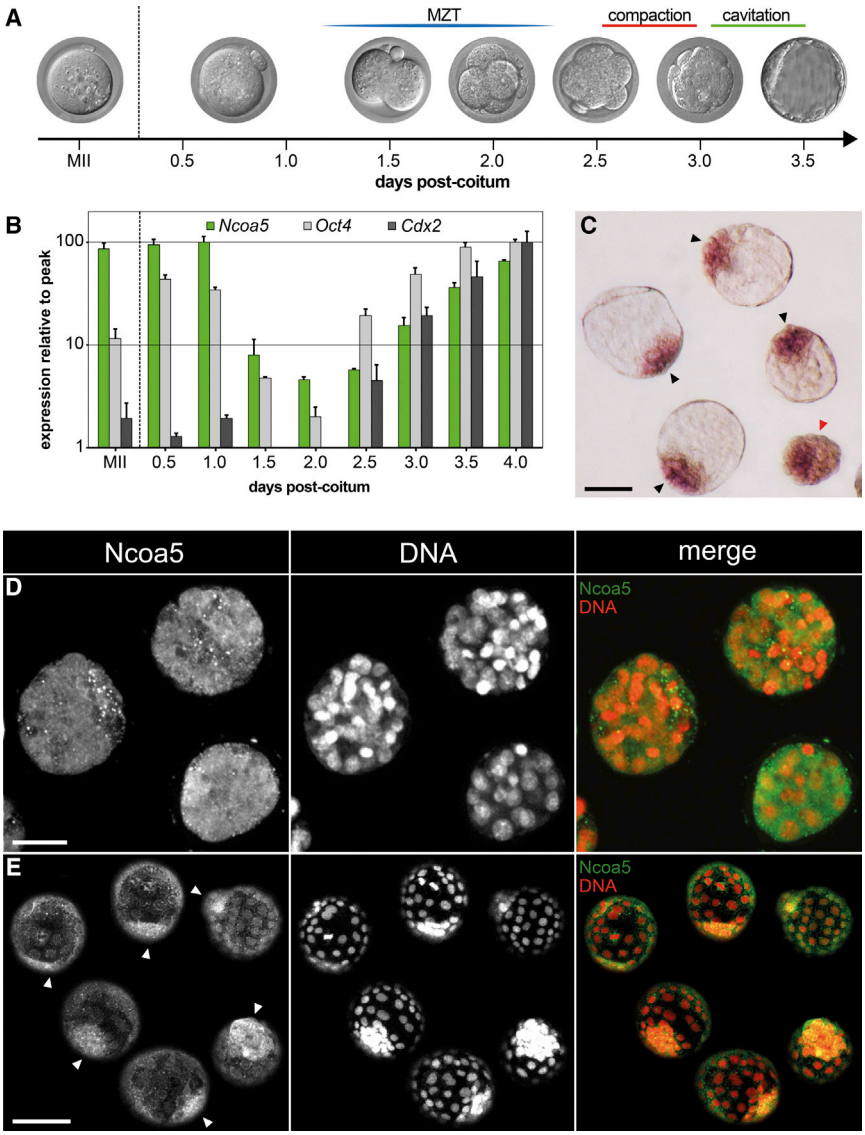

Figure 6. Ncoa5 Is Expressed in Pluripotent Stem Cells of the Mouse Embryo

(A) Mouse preimplantation development. MZT, maternal-to-zygotic transition.

(B) Quantitative real-time PCR of *Ncoa5*, *Oct4*, and *Cdx2* transcripts in embryos collected at different developmental stages. Mean + SEM of three independent experiments is shown.

(C) Whole-mount in situ hybridization of *Ncoa5* transcripts on morulae and blastocysts. Red arrowhead highlights the presence of *Ncoa5* transcripts in all blastomeres of 3.0 morulae, whereas in 4.0 dpc blastocysts expression is restricted to the pluripotent inner cell mass (ICM, black arrowheads).

(D and E) Whole-mount immunostaining of Ncoa5 protein in morulae (D) and blastocysts (E). Ncoa5 is evenly expressed in all blastomeres of 3.0 dpc morulae and localizes to both nucleus and cytoplasm. In 4.0 dpc blastocysts (E), Ncoa5 protein is enriched in the cells of the ICM and its localization is predominantly nuclear (white arrowheads). Scale bars, 80 μm (C and E) and 40 μm (D).

See also Figure S7.

difference in sensitivity might be crucial for the detection of smaller changes of protein levels that accompany biological processes such as regeneration and argues for the use of SILAC in quantitative proteomics.

Comparison of the *Smed* SILAC Stem Cell Proteome with a previously published *Smed* stem cell transcriptome (Solana et al., 2012) revealed that the amount of transcripts detected by RNA-seq is much higher than the one of proteins detected by mass spectrometry (Figure S2B). However, transcriptomic approaches measure the abundance of transcripts but do not consider post-transcriptional changes. As posttranscriptional regulation is an important feature of planarian stem cells (Fernandéz-Taboada et al., 2010; Rouhana et al., 2010, 2012), RNA sequencing gives only a vague estimate regarding the abundance of functionally important proteins.

On a different note, we showed that SILAC proteomics might be helpful in examining planarian protein turnover. Analyzing the $^{13}C_6$-lysine incorporation profile of different proteins during tissue homeostasis indicated that about half of a planarian's protein set is replaced within 4 weeks, including proteins that are almost entirely labeled within the first few days (Figures 1D and S1; Data S1). However, the relatively slow incorporation into other proteins, for example, muscle-resident proteins of the myosin family (Figures 1D and S1), suggests that some proteins, and possibly the cell types they are expressed in, undergo a relatively slow turnover. Thus, our data demonstrate that in vivo SILAC proteomics is a promising tool for the analysis of protein and tissue turnover in planarians.

Notably, we used SILAC proteomics to identify a reproducible set of 394 putative stem cell proteins. Analyzing the expression patterns of 52 of these candidates in planarians with and without stem cells confirmed the stem cell-dependent expression of most of them. This demonstrates that the *Smed* SILAC Stem Cell Proteome is a highly reliable resource, which contains known stem cell regulators and proteins that have not been associated with stem cells before.

Among the 52 tested candidates, we found a putative homolog of mammalian Nuclear Receptor Coactivator 5 (Ncoa5; also known as CIA). Strikingly, RNAi against *ncoa5* caused severe regeneration defects, and eventually death (Figure 4), accompanied by a dramatic loss of the stem cell pool (Figure 5). These phenotypes are similar to genes that have been implicated in the maintenance of the stem cell pool in planarians (Fernandéz-Taboada et al., 2010; Guo et al., 2006; Pearson and Sánchez Alvarado, 2010; Zeng et al., 2013). Consistent with this, stem

cells isolated from *ncoa5* RNAi animals were incapable of repopulating stem cell-depleted host animals (Figure 5E).

What happened to stem cells after *ncoa5* RNAi? Different scenarios could explain the loss of stem cells, including defective proliferation, increased apoptosis, or differentiation. We could exclude a proliferation defect as the major cause, as PH3-positive cells were still present as long as we detected stem cells (Figures 5D, S6B, and S6D). This demonstrated that stem cells were still able to phosphorylate Histone 3 during cell division even in the absence of *ncoa5*. In addition, apoptotic levels appeared to be unaltered after *ncoa5* RNAi (Figures S6C and S6E), indicating that apoptosis was not the major cause of the stem cell loss. Interestingly, RNAi animals could still form a small blastema during the first days of regeneration (Figure 5C), raising the possibility that the existing stem cells behaved normally and were able to differentiate. Hence, we speculate that *ncoa5* RNAi animals might be incapable of replenishing their stem cell pool, possibly due to defective self-renewal.

Interestingly, we found a putative homolog of planarian Ncoa5 expressed in pluripotent stem cells of the mouse embryo (Figures 6 and S7). Mouse *Ncoa5* is maternally contributed and has an early embryonic expression profile similar to the pluripotency gene *Oct4* (Figure 6B). Ncoa5 protein was detected in both trophectodermal cells and in pluripotent cells of the inner cell mass, yet the transcript was only present in the ICM. This suggests that Ncoa5 is specifically induced in pluripotent cells and that Ncoa5 protein in the trophectoderm of 3.5 dpc blastocysts might be a leftover of earlier expression in the morula. This is in line with observations made for Oct4, in which small levels of Oct4 protein result from transcripts expressed in all blastomeres of the morula (Palmieri et al., 1994).

Whether mammalian Ncoa5 is required for the specification and/or the maintenance of a pluripotent stem cell pool in the embryo is currently not clear. We performed *Ncoa5* loss-of-function analysis in the mouse embryo by zygotic siRNA injection. However, whereas RNAi against *Ncoa5* was initially efficient, the knockdown was unstable, and transcript levels recovered to normal as early as 4.5 dpc (Figure S7), indicating that more stable manipulations are required to uncover a role for *Ncoa5* in mammalian embryonic development.

Nonetheless, Ncoa5 is involved in the regulation of Estrogen Receptor alpha-mediated transcription (Sauvé et al., 2001; Zhang and Teng, 2001) and in the expression of *c-Myc* (Jiang et al., 2004), which has been implicated in the control of stem cell self-renewal (Cartwright et al., 2005; Wilson et al., 2004). In addition, the involvement of the Estrogen Receptor Esrrb and its coactivator Ncoa3 in the induction and maintenance of pluripotency (Feng et al., 2009) points toward a role for estrogen-receptor-mediated transcription in pluripotent stem cell function, possibly including additional regulation by Ncoa5.

In summary, we provide a powerful quantitative proteomics method based on metabolic labeling by in vivo SILAC in planarians. We used this method to identify a highly reproducible set of stem cell-associated proteins, the *Smed* SILAC Stem Cell Proteome, and, using the example of Ncoa5, show that SILAC proteomics, in combination with a highly plastic model organism such as planarians, are a powerful tool to identify conserved proteins with putative functions in important biological processes also in mammals. Future applications of SILAC proteomics in planarians might include the global quantification of posttranslational modifications, such as phosphorylation, methylation, or ubiquitination (Monetti et al., 2011; Soldi and Bonaldi, 2013; Udeshi et al., 2012), e.g., during regeneration, or the analysis of protein-protein interactions in more candidate-centric approaches (Selbach and Mann, 2006; Trinkle-Mulcahy et al., 2008). Such experiments could provide important clues on regulatory mechanisms that cannot be captured by transcriptome analyses.

EXPERIMENTAL PROCEDURES

Labeling of Planarians with $^{13}C_6$-Lysine

Asexual planarians of the species *Schmidtea mediterranea* (BCN-10) were labeled with $^{13}C_6$-lysine by feeding them once per week with liver slices from a $^{13}C_6$-lysine labeled mouse (SILAC mouse) (Krüger et al., 2008), a generous gift from Matthias Mann. See text for details.

Sample Preparation for Mass Spectrometry Analysis

Planarians were starved for one week prior to protein extraction. Irradiation was performed in a Gammacell-40 Exactor (Nordion) with two Caesium-137 sources delivering about 0.6 Gy/min. Live animals were exposed to 60 Gy. Proteins were extracted and processed as described in the Supplemental Experimental Procedures.

Mass Spectrometry Analysis and Bioinformatics

LC-MS/MS analysis was performed on a LTQ Orbitrap Velos mass spectrometer, and raw data were processed by MaxQuant software (v1.3.0.5) involving the built-in Andromeda search engine. For details, see the Supplemental Experimental Procedures.

RNAi in Planarians

RNAi was performed as described in Sandmann et al. (2011) but with 1 μg/μl dsRNA solution. In case of a mild phenotype, an additional round of injection and amputation was performed 10 days after the first amputation. Primer sequences are listed in Table S3.

Whole-Mount Immunostaining of Planarians

Immunostainings were performed as described in Cebrià and Newmark (2005) with a rabbit phosphohistone 3 (PH3) antibody (1:600) (Millipore). Nuclear staining was done with Hoechst 33342 (Life Technologies). Images were taken with a Zeiss LSM700 confocal microscope.

In Situ Hybridization on Planarians

Whole-mount in situ hybridization (WISH) with digoxigenin (DIG)-labeled riboprobes was performed as previously described (Nogi and Levin, 2005; Umesono et al., 1999) using the InsituPro VSi hybridization robot (Intavis). Fluorescent whole-mount in situ hybridization (FISH) with either DIG- (Roche) or DNP- (PerkinElmer) labeled riboprobes was performed as described in Pearson et al. (2009). Samples were processed until the blocking step in the InsituPro VSi hybridization robot (Intavis) followed by manual processing, or completely manually. FISH images were taken with a Zeiss LSM700 confocal microscope. Primer sequences are shown in Table S3.

Fluorescent Activated Cell Sorting

Planarian cell dissociation and gating was performed as described in Moritz et al. (2012). FACS analysis was either performed with the Gallios 10/3 Flow Cytometer (Beckman Coulter Genomics) or the FACSAria Cell Sorter (BD Biosciences) and their corresponding software.

Cell Transplantation

Planarian cells from *gfp* or *ncoa5* RNAi animals were dissociated as described above but lacking the Hoechst stain. X1 cells were isolated by FACS. Approximately 1,500 X_1 cells were injected into each lethally irradiated

(~80 Gy) host planarian. Planarians were fixed for double FISH and PH3 immunostaining 7 days post X1 cell injection.

Mice and Embryo Collection

A total of 460 embryos were collected from primed B6 female mice after mating with C3H male mice either 14, 24, 40, 50, 73, or 89 hr after hCG treatment, corresponding to 0.5, 1.0, 1.5, 2.0, 2.5, 3.0, and 3.5 days postcoitum (dpc), respectively. After recovery, embryos were washed three times in M2 medium and either lysed for RNA extraction, or fixed. Some 3.5 dpc blastocysts were cultured overnight in $KSOM^{AA}$ medium at 37°C and 5% CO_2 in air, in order to collect a 4.0 dpc embryonic stage. Mouse work was in accordance with institutional guidelines.

RNA Extraction, cDNA Synthesis, and qPCR of Mouse Tissue

For quantitative analysis of gene expression, embryos were processed as previously described (Boiani et al., 2005), and qPCR was performed using TaqMan chemistry (Life Technologies) for the following genes: *Hprt1* (Mm00446968_m1), *Cdx2* (Mm00432449_m1), and *Oct4* (Mm00658129_gH) (see Table S3 for primer sequences). Three biological replicates were used, and each sample was run with three technical replicates. Data were presented using the percentage of peak method, an adaptation of the $\Delta\Delta C_T$ method (Wang et al., 2004).

Immunostaining of Mouse Embryos and RNAi

siRNAs (GAGUCAAUCUCGAGCAAAAUU; Life Technologies) against mouse *Ncoa5* were microinjected into zygotes as previously described (Wu et al., 2010). Immunofluorescent staining of embryos was performed as described in Strumpf et al. (2005). Polyclonal rabbit anti-mouse Ncoa5 immunoglobulin G (ProteinTech) was used at a concentration of 1:200. Embryos were imaged under a Zeiss LSM700 confocal microscope.

In Situ Hybridization on Mouse Embryos

Ncoa5 transcripts in morulae and blastocysts were detected with 1 μg/ml DIG-labeled *Ncoa5*-specific antisense riboprobe as described previously (Pizard et al., 2004). Embryos were mounted and imaged using an upright microscope (Zeiss).

ACCESSION NUMBERS

The GenBank accession number for *Smed-ncoa5* is KF668097.

SUPPLEMENTAL INFORMATION

Supplemental Information includes Supplemental Experimental Procedures, seven figures, three tables, and seven data files and can be found with this article online at http://dx.doi.org/10.1016/j.celrep.2013.10.035.

ACKNOWLEDGMENTS

We thank S. Zanivan and M. Mann for SILAC mouse liver and advice; S. Pavelka for excellent assistance with mouse experiments; T. Sandmann, D. Eccles, and Y. Perez Rico for bioinformatics assistance; D. Eccles from Gringene Bioinformatics for DEseq analysis; F. Konert for excellent technical assistance; members of the Bartscherer and Gentile laboratories for helpful discussions and comments on the manuscript. The Bartscherer and Schöler laboratories are part of the Cells in Motion (CiM) Cluster of Excellence. H.R. is funded by a stipend from the CiM-IMPRS graduate school. This work was funded by the Max Planck Society and the Deutsche Forschungsgemeinschaft (SFB629, PAK 479).

Received: April 24, 2013
Revised: August 9, 2013
Accepted: October 21, 2013
Published: November 21, 2013

REFERENCES

Adamidi, C., Wang, Y., Gruen, D., Mastrobuoni, G., You, X., Tolle, D., Dodt, M., Mackowiak, S.D., Gogol-Doering, A., Oenal, P., et al. (2011). De novo assembly and validation of planaria transcriptome by massive parallel sequencing and shotgun proteomics. Genome Res. *21*, 1193–1200.

Agata, K., Soejima, Y., Kato, K., Kobayashi, C., Umesono, Y., and Watanabe, K. (1998). Structure of the planarian central nervous system (CNS) revealed by neuronal cell markers. Zoolog. Sci. *15*, 433–440.

Anders, S., and Huber, W. (2010). Differential expression analysis for sequence count data. Genome Biol. *11*, R106.

Baguna, J., Salo, E., and Auladell, C. (1989). Regeneration and Pattern-Formation in Planarians 0.3. Evidence That Neoblasts Are Totipotent Stem-Cells and the Source of Blastema Cells. Development *107*, 77–86.

Berg, J.S., Powell, B.C., and Cheney, R.E. (2001). A millennial myosin census. Mol. Biol. Cell *12*, 780–794.

Blythe, M.J., Kao, D., Malla, S., Rowsell, J., Wilson, R., Evans, D., Jowett, J., Hall, A., Lemay, V., Lam, S., and Aboobaker, A.A. (2010). A dual platform approach to transcript discovery for the planarian Schmidtea mediterranea to establish RNAseq for stem cell and regeneration biology. PLoS ONE *5*, e15617.

Bocchinfuso, D.G., Taylor, P., Ross, E., Ignatchenko, A., Ignatchenko, V., Kislinger, T., Pearson, B.J., and Moran, M.F. (2012). Proteomic profiling of the planarian Schmidtea mediterranea and its mucous reveals similarities with human secretions and those predicted for parasitic flatworms. Mol. Cell. Proteomics *11*, 681–691.

Boiani, M., Gentile, L., Gambles, V.V., Cavaleri, F., Redi, C.A., and Scholer, H.R. (2005). Variable reprogramming of the pluripotent stem cell marker Oct4 in mouse clones: distinct developmental potentials in different culture environments. Stem Cells *23*, 1089–1104.

Bonaldi, T., Straub, T., Cox, J., Kumar, C., Becker, P.B., and Mann, M. (2008). Combined use of RNAi and quantitative proteomics to study gene function in Drosophila. Mol. Cell *31*, 762–772.

Cartwright, P., McLean, C., Sheppard, A., Rivett, D., Jones, K., and Dalton, S. (2005). LIF/STAT3 controls ES cell self-renewal and pluripotency by a Myc-dependent mechanism. Development *132*, 885–896.

Cebrià, F., and Newmark, P.A. (2005). Planarian homologs of netrin and netrin receptor are required for proper regeneration of the central nervous system and the maintenance of nervous system architecture. Development *132*, 3691–3703.

Cox, J., and Mann, M. (2008). MaxQuant enables high peptide identification rates, individualized p.p.b.-range mass accuracies and proteome-wide protein quantification. Nat. Biotechnol. *26*, 1367–1372.

Eisenhoffer, G.T., Kang, H., and Sánchez Alvarado, A. (2008). Molecular analysis of stem cells and their descendants during cell turnover and regeneration in the planarian Schmidtea mediterranea. Cell Stem Cell *3*, 327–339.

Feng, B., Jiang, J., Kraus, P., Ng, J.H., Heng, J.C., Chan, Y.S., Yaw, L.P., Zhang, W., Loh, Y.H., Han, J., et al. (2009). Reprogramming of fibroblasts into induced pluripotent stem cells with orphan nuclear receptor Esrrb. Nat. Cell Biol. *11*, 197–203.

Fernandéz-Taboada, E., Moritz, S., Zeuschner, D., Stehling, M., Schöler, H.R., Saló, E., and Gentile, L. (2010). Smed-SmB, a member of the LSm protein superfamily, is essential for chromatoid body organization and planarian stem cell proliferation. Development *137*, 1055–1065.

Fernández-Taboada, E., Rodríguez-Esteban, G., Saló, E., and Abril, J.F. (2011). A proteomics approach to decipher the molecular nature of planarian stem cells. BMC Genomics *12*, 133.

Forsthoefel, D.J., Park, A.E., and Newmark, P.A. (2011). Stem cell-based growth, regeneration, and remodeling of the planarian intestine. Dev. Biol. *356*, 445–459.

Galloni, M. (2012). Global irradiation effects, stem cell genes and rare transcripts in the planarian transcriptome. Int. J. Dev. Biol. *56*, 103–116.

Gentile, L., Cebrià, F., and Bartscherer, K. (2011). The planarian flatworm: an in vivo model for stem cell biology and nervous system regeneration. Dis. Model. Mech. *4*, 12–19.

Guo, T.X., Peters, A.H.F.M., and Newmark, P.A. (2006). A Bruno-like gene is required for stem cell maintenance in planarians. Dev. Cell *11*, 159–169.

Gygi, S.P., Rochon, Y., Franza, B.R., and Aebersold, R. (1999). Correlation between protein and mRNA abundance in yeast. Mol. Cell. Biol. *19*, 1720–1730.

Hayashi, T., Asami, M., Higuchi, S., Shibata, N., and Agata, K. (2006). Isolation of planarian X-ray-sensitive stem cells by fluorescence-activated cell sorting. Dev. Growth Differ. *48*, 371–380.

Hendzel, M.J., Wei, Y., Mancini, M.A., Van Hooser, A., Ranalli, T., Brinkley, B.R., Bazett-Jones, D.P., and Allis, C.D. (1997). Mitosis-specific phosphorylation of histone H3 initiates primarily within pericentromeric heterochromatin during G2 and spreads in an ordered fashion coincident with mitotic chromosome condensation. Chromosoma *106*, 348–360.

Jiang, C., Ito, M., Piening, V., Bruck, K., Roeder, R.G., and Xiao, H. (2004). TIP30 interacts with an estrogen receptor alpha-interacting coactivator CIA and regulates c-myc transcription. J. Biol. Chem. *279*, 27781–27789.

Kim, J.B., Zaehres, H., Wu, G., Gentile, L., Ko, K., Sebastiano, V., Araúzo-Bravo, M.J., Ruau, D., Han, D.W., Zenke, M., and Schöler, H.R. (2008). Pluripotent stem cells induced from adult neural stem cells by reprogramming with two factors. Nature *454*, 646–650.

Kim, J.B., Sebastiano, V., Wu, G., Araúzo-Bravo, M.J., Sasse, P., Gentile, L., Ko, K., Ruau, D., Ehrich, M., van den Boom, D., et al. (2009). Oct4-induced pluripotency in adult neural stem cells. Cell *136*, 411–419.

Konzer, A., Ruhs, A., Braun, H., Jungblut, B., Braun, T., and Krüger, M. (2013). Stable isotope labeling in zebrafish allows in vivo monitoring of cardiac morphogenesis. Mol. Cell. Proteomics *12*, 1502–1512.

Krijgsveld, J., Ketting, R.F., Mahmoudi, T., Johansen, J., Artal-Sanz, M., Verrijzer, C.P., Plasterk, R.H., and Heck, A.J. (2003). Metabolic labeling of C. elegans and D. melanogaster for quantitative proteomics. Nat. Biotechnol. *21*, 927–931.

Krüger, M., Moser, M., Ussar, S., Thievessen, I., Luber, C.A., Forner, F., Schmidt, S., Zanivan, S., Fässler, R., and Mann, M. (2008). SILAC mouse for quantitative proteomics uncovers kindlin-3 as an essential factor for red blood cell function. Cell *134*, 353–364.

Labbé, R.M., Irimia, M., Currie, K.W., Lin, A., Zhu, S.J., Brown, D.D.R., Ross, E.J., Voisin, V., Bader, G.D., Blencowe, B.J., and Pearson, B.J. (2012). A comparative transcriptomic analysis reveals conserved features of stem cell pluripotency in planarians and mammals. Stem Cells *30*, 1734–1745.

Lapan, S.W., and Reddien, P.W. (2011). dlx and sp6-9 Control optic cup regeneration in a prototypic eye. PLoS Genet. *7*, e1002226.

Liu, Y., Lee, M.R., Timani, K., He, J.J., and Broxmeyer, H.E. (2012). Tip110 maintains expression of pluripotent factors in and pluripotency of human embryonic stem cells. Stem Cells Dev. *21*, 829–833.

Looso, M., Borchardt, T., Krüger, M., and Braun, T. (2010). Advanced identification of proteins in uncharacterized proteomes by pulsed in vivo stable isotope labeling-based mass spectrometry. Mol. Cell. Proteomics *9*, 1157–1166.

McClatchy, D.B., Liao, L., Park, S.K., Venable, J.D., and Yates, J.R. (2007). Quantification of the synaptosomal proteome of the rat cerebellum during post-natal development. Genome Res. *17*, 1378–1388.

Monetti, M., Nagaraj, N., Sharma, K., and Mann, M. (2011). Large-scale phosphosite quantification in tissues by a spike-in SILAC method. Nat. Methods *8*, 655–658.

Moritz, S., Stöckle, F., Ortmeier, C., Schmitz, H., Rodríguez-Esteban, G., Key, G., and Gentile, L. (2012). Heterogeneity of planarian stem cells in the S/G2/M phase. Int. J. Dev. Biol. *56*, 117–125.

Newmark, P.A., and Sánchez Alvarado, A. (2002). Not your father's planarian: a classic model enters the era of functional genomics. Nat. Rev. Genet. *3*, 210–219.

Nogi, T., and Levin, M. (2005). Characterization of innexin gene expression and functional roles of gap-junctional communication in planarian regeneration. Dev. Biol. *287*, 314–335.

Onal, P., Grün, D., Adamidi, C., Rybak, A., Solana, J., Mastrobuoni, G., Wang, Y., Rahn, H.P., Chen, W., Kempa, S., et al. (2012). Gene expression of pluripotency determinants is conserved between mammalian and planarian stem cells. EMBO J. *31*, 2755–2769.

Ong, S.E., Blagoev, B., Kratchmarova, I., Kristensen, D.B., Steen, H., Pandey, A., and Mann, M. (2002). Stable isotope labeling by amino acids in cell culture, SILAC, as a simple and accurate approach to expression proteomics. Mol. Cell. Proteomics *1*, 376–386.

Ong, S.E., and Mann, M. (2005). Mass spectrometry-based proteomics turns quantitative. Nat. Chem. Biol. *1*, 252–262.

Palmieri, S.L., Peter, W., Hess, H., and Schöler, H.R. (1994). Oct-4 transcription factor is differentially expressed in the mouse embryo during establishment of the first two extraembryonic cell lineages involved in implantation. Dev. Biol. *166*, 259–267.

Pearson, B.J., and Sánchez Alvarado, A. (2010). A planarian p53 homolog regulates proliferation and self-renewal in adult stem cell lineages. Development *137*, 213–221.

Pearson, B.J., Eisenhoffer, G.T., Gurley, K.A., Rink, J.C., Miller, D.E., and Sánchez Alvarado, A. (2009). Formaldehyde-based whole-mount in situ hybridization method for planarians. Dev. Dyn. *238*, 443–450.

Pellettieri, J., and Sánchez Alvarado, A. (2007). Cell turnover and adult tissue homeostasis: from humans to planarians. Annu. Rev. Genet. *41*, 83–105.

Pellettieri, J., Fitzgerald, P., Watanabe, S., Mancuso, J., Green, D.R., and Sánchez Alvarado, A. (2010). Cell death and tissue remodeling in planarian regeneration. Dev. Biol. *338*, 76–85.

Percharde, M., Lavial, F., Ng, J.H., Kumar, V., Tomaz, R.A., Martin, N., Yeo, J.C., Gil, J., Prabhakar, S., Ng, H.H., et al. (2012). Ncoa3 functions as an essential Esrrb coactivator to sustain embryonic stem cell self-renewal and reprogramming. Genes Dev. *26*, 2286–2298.

Pizard, A., Haramis, A., Carrasco, A.E., Franco, P., Lopez, S., and Paganelli, A. (2004). Whole-mount in situ hybridization and detection of RNAs in vertebrate embryos and isolated organs. Curr. Protoc. Mol. Biol. *14*, Unit 14.19.

Reddien, P.W. (2013). Specialized progenitors and regeneration. Development *140*, 951–957.

Reddien, P.W., and Sánchez Alvarado, A. (2004). Fundamentals of planarian regeneration. Annu. Rev. Cell Dev. Biol. *20*, 725–757.

Reddien, P.W., Bermange, A.L., Murfitt, K.J., Jennings, J.R., and Sánchez Alvarado, A. (2005a). Identification of genes needed for regeneration, stem cell function, and tissue homeostasis by systematic gene perturbation in planaria. Dev. Cell *8*, 635–649.

Reddien, P.W., Oviedo, N.J., Jennings, J.R., Jenkin, J.C., and Sánchez Alvarado, A. (2005b). SMEDWI-2 is a PIWI-like protein that regulates planarian stem cells. Science *310*, 1327–1330.

Resch, A.M., Palakodeti, D., Lu, Y.C., Horowitz, M., and Graveley, B.R. (2012). Transcriptome analysis reveals strain-specific and conserved stemness genes in Schmidtea mediterranea. PLoS ONE *7*, e34447.

Rothman, S. (2010). How is the balance between protein synthesis and degradation achieved? Theor. Biol. Med. Model. *7*, 25.

Rouhana, L., Shibata, N., Nishimura, O., and Agata, K. (2010). Different requirements for conserved post-transcriptional regulators in planarian regeneration and stem cell maintenance. Dev. Biol. *341*, 429–443.

Rouhana, L., Vieira, A.P., Roberts-Galbraith, R.H., and Newmark, P.A. (2012). PRMT5 and the role of symmetrical dimethylarginine in chromatoid bodies of planarian stem cells. Development *139*, 1083–1094.

Sánchez Alvarado, A., Newmark, P.A., Robb, S.M.C., and Juste, R. (2002). The Schmidtea mediterranea database as a molecular resource for studying platyhelminthes, stem cells and regeneration. Development *129*, 5659–5665.

Sandmann, T., Vogg, M.C., Owlarn, S., Boutros, M., and Bartscherer, K. (2011). The head-regeneration transcriptome of the planarian Schmidtea mediterranea. Genome Biol. *12*, R76.

Sauvé, F., McBroom, L.D., Gallant, J., Moraitis, A.N., Labrie, F., and Giguère, V. (2001). CIA, a novel estrogen receptor coactivator with a bifunctional nuclear receptor interacting determinant. Mol. Cell. Biol. *21*, 343–353.

Schultz, R.M. (2002). The molecular foundations of the maternal to zygotic transition in the preimplantation embryo. Hum. Reprod. Update *8*, 323–331.

Schwanhäusser, B., Gossen, M., Dittmar, G., and Selbach, M. (2009). Global analysis of cellular protein translation by pulsed SILAC. Proteomics *9*, 205–209.

Selbach, M., and Mann, M. (2006). Protein interaction screening by quantitative immunoprecipitation combined with knockdown (QUICK). Nat. Methods *3*, 981–983.

Shibata, N., Hayashi, T., Fukumura, R., Fujii, J., Kudome-Takamatsu, T., Nishimura, O., Sano, S., Son, F.Y., Suzuki, N., Araki, R., et al. (2012). Comprehensive gene expression analyses in pluripotent stem cells of a planarian, Dugesia japonica. Int. J. Dev. Biol. *56*, 93–102.

Solana, J. (2013). Closing the circle of germline and stem cells: the Primordial Stem Cell hypothesis. Evodevo *4*, 2.

Solana, J., Kao, D., Mihaylova, Y., Jaber-Hijazi, F., Malla, S., Wilson, R., and Aboobaker, A. (2012). Defining the molecular profile of planarian pluripotent stem cells using a combinatorial RNAseq, RNA interference and irradiation approach. Genome Biol. *13*, R19.

Soldi, M., and Bonaldi, T. (2013). The proteomic investigation of chromatin functional domains reveals novel synergisms among distinct heterochromatin components. Mol. Cell. Proteomics *12*, 764–780.

Strumpf, D., Mao, C.A., Yamanaka, Y., Ralston, A., Chawengsaksophak, K., Beck, F., and Rossant, J. (2005). Cdx2 is required for correct cell fate specification and differentiation of trophectoderm in the mouse blastocyst. Development *132*, 2093–2102.

Sury, M.D., Chen, J.X., and Selbach, M. (2010). The SILAC fly allows for accurate protein quantification in vivo. Mol. Cell. Proteomics *9*, 2173–2183.

Takahashi, K., Tanabe, K., Ohnuki, M., Narita, M., Ichisaka, T., Tomoda, K., and Yamanaka, S. (2007). Induction of pluripotent stem cells from adult human fibroblasts by defined factors. Cell *131*, 861–872.

Trinkle-Mulcahy, L., Boulon, S., Lam, Y.W., Urcia, R., Boisvert, F.M., Vandermoere, F., Morrice, N.A., Swift, S., Rothbauer, U., Leonhardt, H., and Lamond, A. (2008). Identifying specific protein interaction partners using quantitative mass spectrometry and bead proteomes. J. Cell Biol. *183*, 223–239.

Udeshi, N.D., Mani, D.R., Eisenhaure, T., Mertins, P., Jaffe, J.D., Clauser, K.R., Hacohen, N., and Carr, S.A. (2012). Methods for quantification of in vivo changes in protein ubiquitination following proteasome and deubiquitinase inhibition. Mol. Cell. Proteomics *11*, 148–159.

Umesono, Y., Watanabe, K., and Agata, K. (1999). Distinct structural domains in the planarian brain defined by the expression of evolutionarily conserved homeobox genes. Dev. Genes Evol. *209*, 31–39.

Wagner, D.E., Wang, I.E., and Reddien, P.W. (2011). Clonogenic neoblasts are pluripotent adult stem cells that underlie planarian regeneration. Science *332*, 811–816.

Wagner, D.E., Ho, J.J., and Reddien, P.W. (2012). Genetic regulators of a pluripotent adult stem cell system in planarians identified by RNAi and clonal analysis. Cell Stem Cell *10*, 299–311.

Wang, Q.T., Piotrowska, K., Ciemerych, M.A., Milenkovic, L., Scott, M.P., Davis, R.W., and Zernicka-Goetz, M. (2004). A genome-wide study of gene activity reveals developmental signaling pathways in the preimplantation mouse embryo. Dev. Cell *6*, 133–144.

Wenemoser, D., and Reddien, P.W. (2010). Planarian regeneration involves distinct stem cell responses to wounds and tissue absence. Dev. Biol. *344*, 979–991.

Westman-Brinkmalm, A., Abramsson, A., Pannee, J., Gang, C., Gustavsson, M.K., von Otter, M., Blennow, K., Brinkmalm, G., Heumann, H., and Zetterberg, H. (2011). SILAC zebrafish for quantitative analysis of protein turnover and tissue regeneration. J. Proteomics *75*, 425–434.

Wilson, A., Murphy, M.J., Oskarsson, T., Kaloulis, K., Bettess, M.D., Oser, G.M., Pasche, A.C., Knabenhans, C., Macdonald, H.R., and Trumpp, A. (2004). c-Myc controls the balance between hematopoietic stem cell self-renewal and differentiation. Genes Dev. *18*, 2747–2763.

Wu, G., Gentile, L., Fuchikami, T., Sutter, J., Psathaki, K., Esteves, T.C., Araúzo-Bravo, M.J., Ortmeier, C., Verberk, G., Abe, K., and Schöler, H.R. (2010). Initiation of trophectoderm lineage specification in mouse embryos is independent of Cdx2. Development *137*, 4159–4169.

Wu, Z.T., Yang, M., Liu, H.J., Guo, H.C., Wang, Y., Cheng, H., and Chen, L.Y. (2012). Role of nuclear receptor coactivator 3 (Ncoa3) in pluripotency maintenance. J. Biol. Chem. *287*, 38295–38304.

Zeng, A., Li, Y.Q., Wang, C., Han, X.S., Li, G., Wang, J.Y., Li, D.S., Qin, Y.W., Shi, Y.F., Brewer, G., and Jing, Q. (2013). Heterochromatin protein 1 promotes self-renewal and triggers regenerative proliferation in adult stem cells. J. Cell Biol. *201*, 409–425.

Zhang, Z.P., and Teng, C.T. (2001). Estrogen receptor alpha and estrogen receptor-related receptor alpha1 compete for binding and coactivator. Mol. Cell. Endocrinol. *172*, 223–233.